

## Water Dimer Radical Cation: Structures, Vibrational Frequencies, and Energetics

Qianyi Cheng, Francesco A. Evangelista, Andrew C. Simmonett, Yukio Yamaguchi, and Henry F. Schaefer III\*

Center for Computational Quantum Chemistry, University of Georgia, Athens, Georgia, 30602-2525

Received: August 10, 2009; Revised Manuscript Received: October 13, 2009

Fourteen stationary points for the water dimer radical cation on its doublet electronic state potential energy surface have been characterized using coupled cluster theory with single and double excitations (CCSD) and CCSD with perturbative triple excitations [CCSD(T)]. This is done in conjunction with Dunning's correlation consistent polarized valence basis sets (cc-pVXZ and aug-cc-pVXZ,  $X = D, T, Q$ ). Two stationary points are found to be local minima, isomer **1** ( $C_1$  symmetry) with  $H_3O^+ \cdots OH$  character (hydrogen-bonded system), and isomer **7** ( $C_2$  symmetry) with  $[H_2O \cdots H_2O]^+$  character (hemibonded system). Among the other stationary points, seven are transition states, and the remaining five are higher order saddle points. The fourteen water dimer radical cation structures lie within 45 kcal mol<sup>-1</sup> of isomer **1**. Structure **1**, transition states **2** ( $C_s$  symmetry) and **3** ( $C_s$  symmetry) are related through torsion of the OH group; these three stationary points fall within one kcal mol<sup>-1</sup>, demonstrating the low energy barrier of the OH torsional mode. Adiabatic ionization energies of  $(H_2O)_2$  to **1** and **7** are determined to be 10.81 and 11.19 eV, respectively; the former is in excellent agreement with the experimental value of 10.8–10.9 eV. The critical dissociation energy of **1** to  $H_3O^+ + OH^{\cdot}$  is predicted to be 26.4 kcal mol<sup>-1</sup>, while the dissociation energy of isomer **7** to  $H_2O^+ + H_2O$  is determined to be 34.7 kcal mol<sup>-1</sup>. At the aug-cc-pVQZ CCSD(T) level of theory, the hydrogen-bonded **1** and hemibonded **7** minima are separated by 8.8 kcal mol<sup>-1</sup> with an interconversion barrier (**1** → **10** → **7**) of 15.1 kcal mol<sup>-1</sup>. A careful comparison is made with the recent experiments of Gardenier, Johnson, and McCoy on  $(H_2O)_2^+ \cdot Ar$  and  $(H_2O)_2^+ \cdot Ar_2$ .

## I. Introduction

Dynamical simulations and computations of the bulk properties of liquids<sup>1,2</sup> become computationally tractable when energies and forces are obtained from inexpensive methods, such as molecular mechanics, semiempirical theory, or density functional theory (DFT). In molecular mechanics, force fields are often constructed to perform well for a specific problem; in this process, ab initio information is often used to impose constraints on the parametrization. Even when employing density functional theory, the choice of a specific functional is usually made based upon comparisons to ab initio results. For both of these purposes, reference data on small model systems is typically employed.

Given the ubiquity of water in biological processes, it is no surprise that small water clusters<sup>3–8</sup> have been investigated extensively. These studies include the characterization of electron attachment and localization modes (surface and interior states) in water clusters,<sup>4–6,9</sup> ionized clusters,<sup>1,2,10–21</sup>  $(H_2O)_n^-$ ,  $(H_2O)_n^+$ , and fragmentation processes occurring upon ionization,<sup>15,22–27</sup> as well as studies of ion and neutral hydration systems,<sup>15,22,28–30</sup> that is,  $X(H_2O)_n$  and  $X(H_2O)_n^{\pm}$ , where X is a solvated species (atom or molecule), including the protonated clusters  $(H_2O)_nH^+$ .<sup>7,15,22,28,31–33</sup> The fascinating rearrangement dynamics of hydrogen-bond networks and unique proton transfer mechanisms in water have led to myriad experimental studies.<sup>11,12,20,27,30,34,35</sup>

Experiments on water clusters have primarily focused on neutral molecules, hydrated electron clusters<sup>36–43</sup> and protonated cluster ions  $(H_2O)_nH^+$ . Protonated clusters exhibit very rich and varied chemistry, such as electron transfer, proton transfer, and molecular rearrangement. The smallest of these clusters,

$(H_2O)_2H^+$ , plays an important role in the ion chemistry of the upper atmosphere, dominating the ion composition in the D region in the ionosphere.<sup>44</sup> Furthermore, oxonium ions such as  $H_3O^+$  and  $H_5O_2^+$  occur as solvated charge carriers in aqueous solutions, condensed phases (ices), and clusters such as  $(H_2O)_{21}H^+$  [often referred as  $(H_2O)_{20} \cdot H_3O^+$ , an oxonium hydrated in a cage of 20 water molecules].<sup>45</sup> These charged water species have been investigated experimentally and theoretically.<sup>1,2,15,18,22,26,27</sup>

In contrast, much less work has been done on the electronic and molecular structures of corresponding radical cation clusters  $(H_2O)_n^+$ , which are, for example, generated in vivo by water radiolysis. Early photoionization studies<sup>12</sup> of neutral water dimer detected a low signal of  $(H_2O)_2^+$  near threshold and determined an upper bound of the dimer adiabatic ionization potential (aIP) [ $(H_2O)_2$ ]  $\leq 11.21 \pm 0.09$  eV; a lower value of 10.81–10.90 eV has also been suggested.<sup>14</sup> Later He I photoelectron measurements<sup>34</sup> determined the vertical ionization potential (vIP) [ $(H_2O)_2$ ] =  $12.1 \pm 0.1$  ( $^2A''$  state) and  $13.2 \pm 0.2$  eV ( $^2A'$  state). Shinohara et al.<sup>11</sup> observed unprotonated  $(H_2O)_n^+$  clusters ( $2 \leq n \leq 10$ ) for the first time by applying near threshold photoionization with an Ar resonance lamp (11.83 eV) for a molecular beam expansion of  $H_2O$  and Ar. Recently, Dong<sup>35</sup> detected a small signal for  $(H_2O)_2^+$ , the daughter ion for  $(H_2O)_3$ , using a soft X-ray laser. These experiments suggest that the exiting electron removes almost all of the excess energy in these clusters. The difficulty of observing  $(H_2O)_n^+$  clusters is attributed<sup>26,46</sup> to the large configurational differences between the parent neutrals and the ionized clusters, which result in small Franck–Condon factors for the ionization process.<sup>47–49</sup> Consequently, the vertically ionized cluster is formed in a highly vibrationally excited state, leading to dissociation.<sup>47,50,51</sup> Dis-

\* To whom correspondence should be addressed. E-mail: sch@uga.edu.

sociation of the neutral water dimer may occur via two alternative channels:<sup>26</sup> the “oxonium channel”  $[(\text{H}_2\text{O})_2 + h\nu \rightarrow \text{H}_3\text{O}^+ + \text{OH} + e^-]$ , and the “water channel”  $[(\text{H}_2\text{O})_2 + h\nu \rightarrow \text{H}_2\text{O}^+ + \text{H}_2\text{O} + e^-]$ . In 2009, Gardenier and co-workers<sup>27</sup> reported a spectroscopic study of the ion-radical hydrogen-bonded  $\text{H}_4\text{O}_2^+$ . Based on the pattern of infrared transitions, it was unambiguously established that this species is best described as the  $\text{H}_3\text{O}^+\cdots\text{OH}^+$  ion-radical complex.

Early theoretical studies<sup>48,52</sup> of the neutral water dimer reported 10 stationary point structures (all with  $\text{H}_2\text{O}\cdots\text{H}_2\text{O}$  character), at the second- and fourth-order Møller–Plesset levels of theory.<sup>52</sup> Later, coupled cluster with single and double excitations (CCSD) as well as CCSD with perturbative triple excitations [CCSD(T)] were employed to refine the structures.<sup>48</sup> The 10 structures include one minimum (nonplanar open  $C_s$ ), three transition states (open  $C_1$ , cyclic  $C_i$ , and nonplanar bifurcated  $C_{2v}$ ), and six higher order saddle points. The energy barriers connecting these structures range from 0.52 to 1.79 kcal mol<sup>-1</sup>.

The water dimer radical cation  $(\text{H}_2\text{O})_2^+$  has also been studied theoretically.<sup>53–55</sup> Two different structures can result from ionization of the neutral; one is the oxonium-like complex  $\text{H}_3\text{O}^+\cdots\text{OH}$ , and the other is the water-like complex  $[\text{H}_2\text{O}\cdots\text{H}_2\text{O}]^+$ . In 1987, Gill and Radom characterized the  $^2A'$  state of the hydrogen-bonded ( $C_s$  symmetry) isomer and the  $^2B_u$  state of the hemibonded ( $C_{2h}$  symmetry) isomer as two minima at the MP4/6-311G(MC)\*\*//MP2/6-31G\* level of theory.<sup>56</sup> The energy difference between the two isomers was found to be 8.9 kcal mol<sup>-1</sup>. Sodupe, Oliva, and Bertran located five structures<sup>57</sup> of the ionized water dimer  $(\text{H}_2\text{O})_2^+$ , including two  $C_1$  minima (one hydrogen-bonded structure and one hemibonded structure) and three transition states (two  $^2A'$  states for the  $C_s$  hemibonded isomers and one  $^2A''$  state for the  $C_s$  hydrogen-bonded isomer) at the MCPF/TZ2P++//MP2/TZ2P++ level of theory.<sup>57</sup> In Sodupe's paper, the  $C_s$  symmetry transition state was found to be similar to the  $C_1$  minimum structure, but with the OH rotated out of the plane. The energy difference between these two structures was predicted to be 0.03 kcal mol<sup>-1</sup>. The vertical ionization energies of the water dimer were computed to be 11.5 and 12.9 eV for the  $^2A''$  and  $^2A'$  states, respectively.

In the present research, a systematic theoretical study employing the CCSD and CCSD(T) levels of theory is carried out to investigate the molecular and electronic structures of the water dimer radical cations. The purpose of our research is to characterize the structures of the fourteen stationary points on the electronic doublet potential energy surface (PES) and to examine the dissociation pathways of ionized water dimers. Furthermore, newly determined structures and binding energies will be compared with previous studies<sup>48,52</sup> of the neutral water dimer and water dimer radical cations.<sup>56,57</sup> Our results will hopefully serve as benchmarks, against which more approximate models can be calibrated.

## II. Theoretical Methods

The geometries of the water dimer and the different water dimer radical cation structures were optimized at the unrestricted coupled cluster with single and double excitations (UCCSD)<sup>58–60</sup> and UCCSD with a perturbative approximation of triple excitations [UCCSD(T)]<sup>58,61,62</sup> levels of theory. However, restricted open-shell Hartree–Fock (ROHF) wave functions were used as a reference. Structures of neutral water dimers and water dimer radical cations discussed previously<sup>48,52,56,57</sup> were used as starting points for geometry optimizations. Dunning's correlation-consistent polarized valence basis sets (cc-

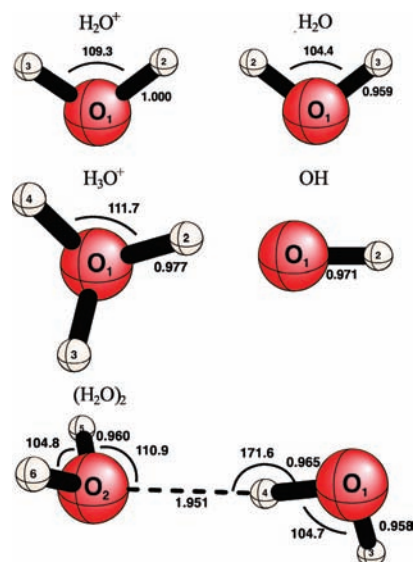


**Figure 1.** Geometries of the water radical cation, water, hydronium, hydroxyl radical, and the neutral water dimer predicted at the CCSD(T) level of theory using the aug-cc-pVQZ basis set. Bond distances are in angstroms and bond angles in degrees.

pVXZ and aug-cc-pVXZ, where  $X = \text{D, T, Q}$ )<sup>63,64</sup> were employed. The harmonic vibrational frequencies of stationary points were determined via numerical differentiation of total energies. Second order Møller–Plesset perturbation theory (MP2)<sup>65</sup> was employed in the intrinsic reaction coordinate (IRC) analysis.

The computations were carried out using QChem 3.1,<sup>66</sup> Molpro 2006.1,<sup>67</sup> the Mainz–Austin–Budapest (MAB) version of ACESII,<sup>68,69</sup> and PSI3.<sup>70</sup>

## III. Results and Discussion

**A. Structural Analyses.** The optimized structures of the neutral water dimer and the fourteen stationary points (**1–14**, numbered in order of increasing energy) of the water dimer radical cation [at the aug-cc-pVQZ CCSD(T) level of theory] are displayed in Figures 1–4 and Table 1. The Cartesian coordinates (in bohr) of the water dimer radical cation stationary points at aug-cc-pVQZ CCSD(T) level of theory discussed herein are available as Supporting Information.

These fourteen  $(\text{H}_2\text{O})_2^+$  stationary points may be classified in the following three categories: Group A ( $\text{H}_2\text{O}-\text{H}^+\cdots\text{OH}$ ) – proton transferred structures (**1–5**) with a bridging hydrogen, Group B ( $\text{H}_3\text{O}^+\cdots\text{OH}$ ) – proton transferred structures (**6** and **9**) without the hydrogen bridge, and Group C ( $[\text{H}_2\text{O}\cdots\text{H}_2\text{O}]^+$ ) – hemibonded structures (**7, 8, 10–14**). For the proton-transferred ( $\text{H}_3\text{O}^+\cdots\text{OH}$ ) complex, the positive charge lies mainly on the  $\text{H}_3\text{O}^+$  fragment, while for the hemibonded ( $[\text{H}_2\text{O}\cdots\text{H}_2\text{O}]^+$ ) complex, the positive charge is delocalized between the two monomers.

**1. Group A.** Structures **1–5** (shown in Figure 2) all fall into group A as a result of their connectivity, but have different orientations of the OH group. Among these five structures isomer **1** is the global minimum on the doublet electronic ground state PES, while **2** and **3** are transition states connecting mirror images of **1** via OH torsion. Structures **4** and **5** are analogous to **1–3**, but with different symmetry constraints imposed. Comparing the neutral water dimer global minimum ( $^1A'$   $C_s$ ) and the water dimer radical cation **1** ( $^2A'$   $C_1$ ) structure, there are significant geometrical changes:

(1) the symmetry of the dimer is lowered from  $C_s$  to  $C_1$  upon ionization;

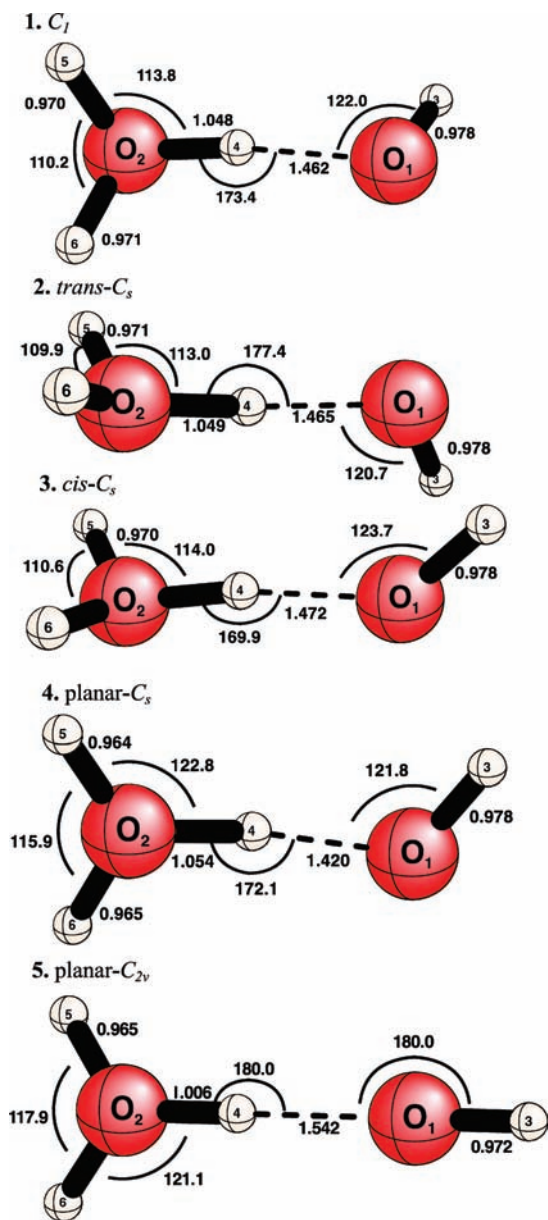


**Figure 2.** Geometries of the water dimer radical cation structures 1–5 predicted at the CCSD(T) level of theory using the aug-cc-pVQZ basis set. Bond distances are in angstroms and bond angles in degrees.

(2) the hydrogen bond (H-bond) is slightly closer to linearity for the dimer radical cation [ $\theta_e(\text{OH}\cdots\text{O}) = 173.4^\circ$ ] than for the neutral [ $\theta_e(\text{OH}\cdots\text{O}) = 171.6^\circ$ ];

(3) the oxygen–oxygen distance of the dimer radical cation [ $r_e(\text{O}_1\cdots\text{O}_2) = 2.506 \text{ \AA}$ ] is shorter than that of the neutral [ $r_e(\text{O}_1\cdots\text{O}_2) = 2.910 \text{ \AA}$ ];

(4) the H-bonded OH bond distance for the dimer radical cation [ $r_e(\text{O}_2\text{H}_4) = 1.048 \text{ \AA}$ ] is longer than that for the neutral [ $r_e(\text{O}_1\text{H}_4) = 0.965 \text{ \AA}$ ];

(5) the non H-bonded OH bond distances for the dimer radical cation [ $r_e(\text{O}_2\text{H}_5) \approx r_e(\text{O}_2\text{H}_6) = 0.971 \text{ \AA}$ ] are longer than those of the neutral water dimer [ $r_e(\text{O}_2\text{H}_5) = r_e(\text{O}_2\text{H}_6) = 0.960 \text{ \AA}$ ], but shorter than that of the isolated  $\text{H}_3\text{O}^+$  cation [ $r_e(\text{OH}) = 0.977 \text{ \AA}$ ];

(6) the non H-bonded OH bond distance of the dimer radical cation [ $r_e(\text{O}_1\text{H}_3) = 0.978 \text{ \AA}$ ] is elongated compared to those of the isolated OH radical [ $r_e(\text{OH}) = 0.971 \text{ \AA}$ ] and especially the neutral dimer [ $r_e(\text{O}_1\text{H}_3) = 0.958 \text{ \AA}$ ];

(7) the non H-bonded HOH bond angle for the  $(\text{H}_2\text{O})_2^+$  radical cation [ $\theta_e(\text{H}_3\text{O}_2\text{H}_6) = 110.2^\circ$ ] is larger than that for the

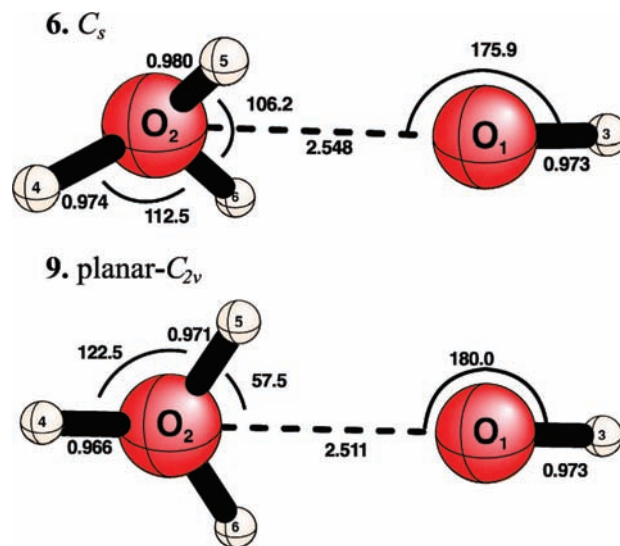


**Figure 3.** Geometries of the water dimer radical cation structures 6 and 9 predicted at the CCSD(T) level of theory using the aug-cc-pVQZ basis set. Bond distances are in angstroms and bond angles in degrees.

neutral  $(\text{H}_2\text{O})_2$  [ $\theta_e(\text{H}_3\text{O}_2\text{H}_6) = 104.8^\circ$ ], but smaller than that for the isolated  $\text{H}_3\text{O}^+$  cation [ $\theta_e(\text{HOH}) = 111.7^\circ$ ].

**2. Group B.** Structure 6 and 9 (shown in Figure 3) are similar to the group A structures because of their proton transferred nature, but lack a hydrogen bond. These structures are not minima on the potential energy surface.

**3. Group C.** All seven structures in group C (shown in Figure 4) lack hydrogen bonding between the two  $\text{H}_2\text{O}$  units; they are instead hemibonded complexes. Of all group C structures, only 7, which possesses  $C_2$  symmetry, is a local minimum. Comparing the water dimer radical cation 7, to the neutral water monomer  $\text{H}_2\text{O}$ , and the isolated water radical cation  $\text{H}_2\text{O}^+$ , there are some notable geometric differences due to complexation:

(1) the OH bond distance for the dimer radical cation 7 [ $r_e(\text{OH}) = 0.977 \text{ \AA}$ ] is in-between those for  $\text{H}_2\text{O}$  [ $r_e(\text{OH}) = 0.959 \text{ \AA}$ ] and  $\text{H}_2\text{O}^+$  [ $r_e(\text{OH}) = 1.000 \text{ \AA}$ ];

(2) the HOH bond angle for the dimer radical cation 7 [ $\theta_e(\text{HOH}) = 105.7^\circ$ ] is in-between those for  $\text{H}_2\text{O}$  [ $\theta_e(\text{HOH}) = 104.4^\circ$ ] and  $\text{H}_2\text{O}^+$  [ $\theta_e(\text{HOH}) = 109.3^\circ$ ].

The water dimer radical cation 10 is the isomerization transition state connecting 1 and 7. The transition from 1 to 7 primarily involves the transfer of hydrogen atom 4 from  $\text{O}_1$  to  $\text{O}_2$ , followed by a rotation of the  $\text{H}_3\text{—O}_1\text{—H}_4$  subunit. To trace the path of this proton transfer reaction within the water dimer radical cation, the intrinsic reaction coordinate (IRC) method was adopted using the aug-cc-pVDZ MP2 method. The schematic potential energy surface (in  $\text{kcal mol}^{-1}$ ) is shown pictorially in Figure 5, where selected geometries along the intrinsic reaction coordinate (IRC) between 1, 10 and 7 are included. By starting at the transition structure 10 and following the line of steepest descent in the metric of mass-weighted coordinates we confirm that 10 does, indeed, connect structures 1 and 7. The reaction path shows the hydrogen donor water fragment of the minimum  $C_2$  rotates one of its hydrogen atoms toward the hydrogen acceptor water, and rotates another hydrogen away from the acceptor, which connects to the transition state 10. Then the inner hydrogen moves all the way to the oxygen of the hydrogen acceptor water, which connects to the global minimum 1.

The other five stationary points in category C were located on the PES using symmetry constraints to the structure.

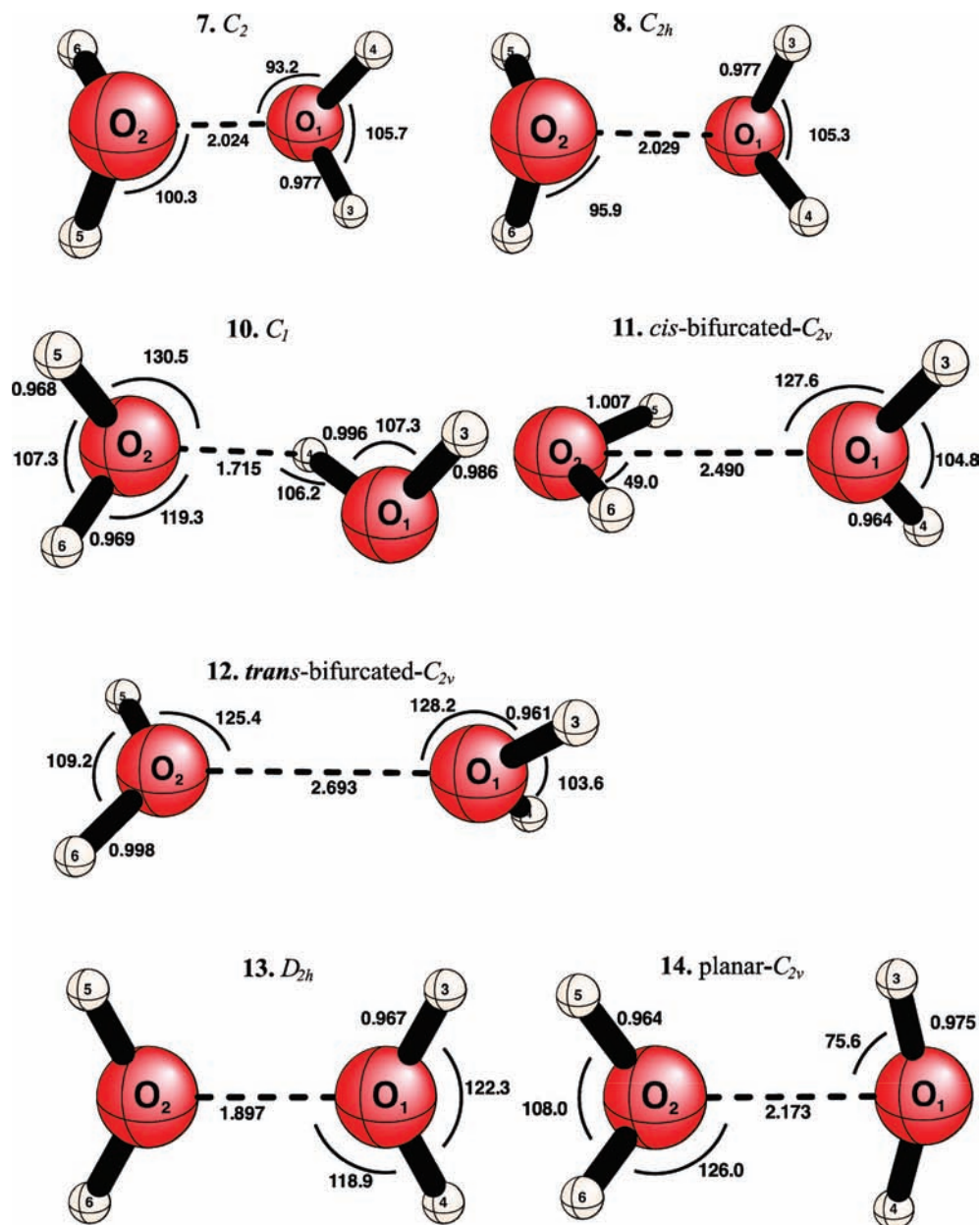


**Figure 4.** Geometries of the water dimer radical cation structures 7, 8, and 10–14 predicted at the CCSD(T) level of theory using the aug-cc-pVQZ basis set. Bond distances are in angstroms and bond angles in degrees.

**TABLE 1: Optimized Geometrical Parameters of  $(\text{H}_2\text{O})_2$  and the Fourteen Stationary Points of  $(\text{H}_2\text{O})_2^+$  at the aug-cc-pVQZ CCSD(T) Level of Theory<sup>a</sup>**

structure	$r_{\text{O}_1\text{O}_2}$	$r_{\text{O}_2\text{H}_4}$	$\theta_{\text{O}_2\text{H}_4\text{O}_1}$	$\theta_{\text{H}_3\text{O}_2\text{H}_4}$	$\tau_{\text{H}_4\text{O}_1\text{O}_2\text{H}_3}$	$\tau_{\text{H}_4\text{O}_1\text{O}_2\text{H}_3}$	$\tau_{\text{H}_6\text{O}_1\text{O}_2\text{H}_4}$
1 $(\text{H}_2\text{O})_2 C_s$	2.910	1.951	171.6	110.9	0.0	122.9	-122.9
2 $C_1$	2.506	1.048	173.4	112.8	-39.7	-154.5	-28.3
3 <i>trans</i> - $C_s$	2.513	1.049	177.4	113.0	0.0	117.8	-117.8
4 <i>cis</i> - $C_s$	2.508	1.046	169.9	114.0	0.0	-66.6	66.6
5 planar $C_s$	2.469	1.054	172.1	122.8	0.0	0.0	180.0
6 planar $C_{2v}$	2.548	1.006	180.0	121.1	0.0		
7 $C_s$	2.548	0.974	30.3	112.5	180.0	-83.3	83.3
8 $C_2$	2.024	2.296	61.7	123.0	106.6	-156.7	96.8
9 $C_{2h}$	2.029	2.342	59.5	120.5	106.2	180.0	73.8
10 planar $C_{2v}$	2.511	0.966	0.0	122.5	0.0		
11 $C_1$	2.210	1.715	106.2	130.5	104.5	-133.7	118.4
12 <i>cis</i> -bifurcated $C_{2v}$	2.505	3.172	38.5	50.4	180.0	90.0	-90.0
13 <i>trans</i> -bifurcated $C_{2v}$	2.693	3.373	38.8	124.4	180.0	90.0	-90.0
14 $D_{2h}$	1.897	2.511	41.4	138.6	180.0	180.0	0.0
15 planar $C_{2v}$	2.173	2.150	78.3	152.0	180.0	180.0	0.0

<sup>a</sup> Bond lengths are in angstroms; bond angles and dihedral angles are in degrees.

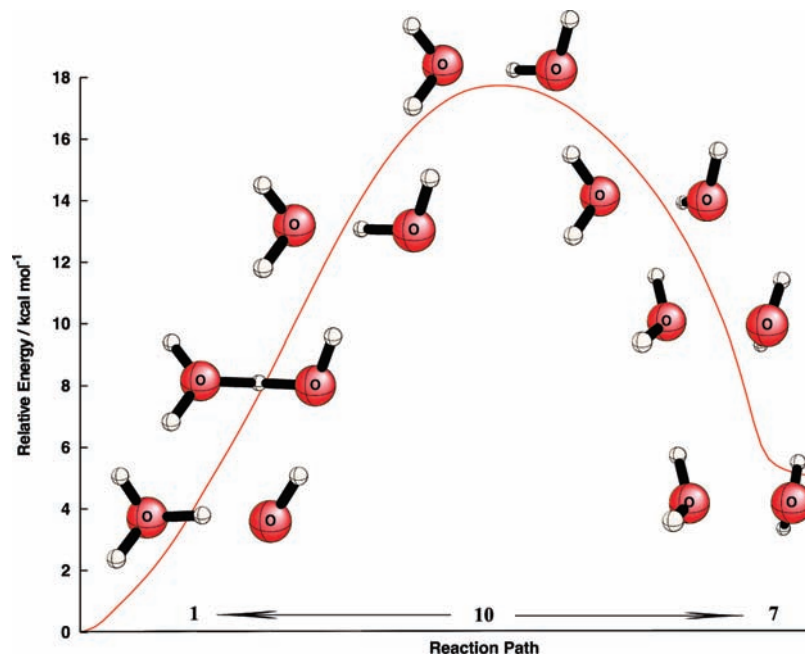


**Figure 5.** Intrinsic reaction coordinate (IRC) for the proton-transfer process involving water dimer radical cation structures **1**, **7**, and **10** at the aug-cc-pVDZ MP2 level of theory.

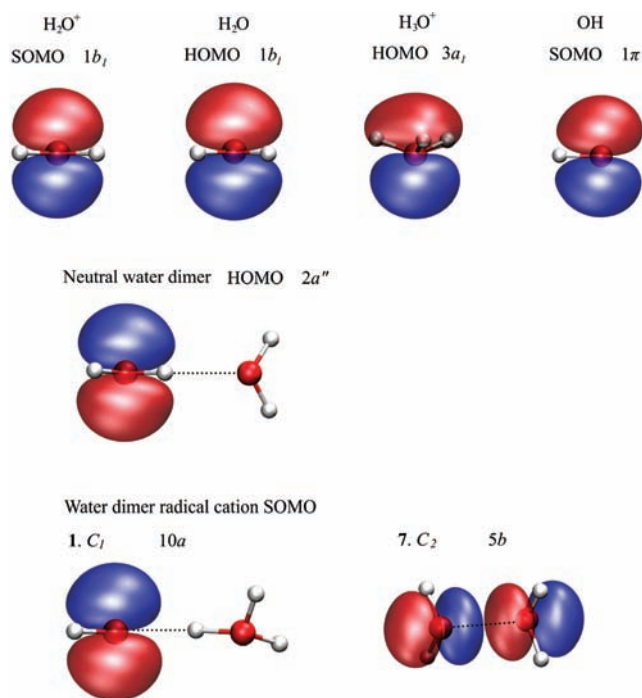
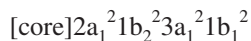


**Figure 6.** Singly occupied molecular orbitals (SOMO) of  $\text{H}_2\text{O}^+$ ,  $\text{OH}$ , and the  $(\text{H}_2\text{O})_2^+$  equilibria **1** and **7**. Also shown are the highest occupied molecular orbitals (HOMO) of  $\text{H}_2\text{O}$ ,  $\text{H}_3\text{O}^+$ , and the  $(\text{H}_2\text{O})_2$ .

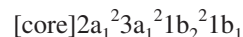
## B. Electron Configurations and Charge Distribution.

**1. Electron Configurations of Standard  $\text{H}_2\text{O}$ ,  $\text{H}_2\text{O}^+$ ,  $(\text{H}_2\text{O})_2$  and Vertical Ionized States of  $(\text{H}_2\text{O})_2$ .** The highest occupied molecular orbitals (HOMO) of  $\text{H}_2\text{O}$ ,  $\text{H}_3\text{O}^+$ , and  $(\text{H}_2\text{O})_2$ , and the singly occupied molecular orbital (SOMO) of  $\text{H}_2\text{O}^+$  and  $\text{OH}\cdot$  are shown in Figure 6.

The ground electronic state of the  $\text{H}_2\text{O}$  monomer  $\tilde{X}^1A_1 (C_{2v})$  has the electron configuration

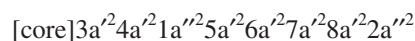


where [core] denotes the lowest-lying core [O: 1s-like] orbital  $1a_1$ . The highest occupied molecular orbital (HOMO)  $1b_1$  is predominantly the 2p (out of plane orbital) of the O atom. The ground electronic state of the  $\text{H}_2\text{O}^+$   $\tilde{X}^2B_1 (C_{2v})$  has the electron configuration



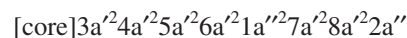
where the singly occupied molecular orbital (SOMO) is the  $1b_1$  orbital (2p of the oxygen atom) as mentioned above.

The ground electronic state of the neutral water dimer  $(\text{H}_2\text{O})_2$   $\tilde{X}^1A'$  ( $C_s$ ) has the electron configuration

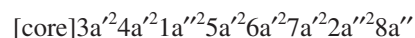


where [core] denotes the two lowest-lying core [O: 1s-like] orbitals  $1a'$  and  $2a'$ . The  $7a'$  orbital represents the in-plane O–H bonding orbital which is formed from the proton donor  $3a_1$  orbital and the proton acceptor  $1b_1$  orbital. The  $8a'$  orbital mainly consists of the  $\text{O}_2$  oxygen 2p orbital in the  $C_s$  plane, while the  $2a''$  (HOMO) orbital represents the  $\text{O}_1$  oxygen 2p orbital perpendicular to the  $C_s$  plane. The orbital energy of the  $8a'$  orbital ( $-0.53$  hartree at the aug-cc-pVQZ RHF level) is significantly lower than that of the  $2a''$  orbital ( $-0.48$  hartree at the same level).

The lowest energy  $\tilde{X}^2A'' (C_s)$  vertical ionized state of the neutral water dimer has the following electron configuration



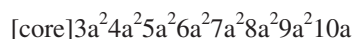
where the  $8a'$  and  $2a''$  (SOMO) orbital energies are  $-0.72$  and  $-0.66$  hartree at the aug-cc-pVQZ ROHF level, whereas the  $\tilde{A}^2A' (C_s)$  vertical ionized state of the  $(\text{H}_2\text{O})_2$  has the electron configuration



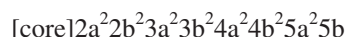
where the  $2a''$  and  $8a'$  (SOMO) orbital energies are  $-0.93$  and  $-0.73$  hartree at the same level of theory.

**2. Electron Configurations of the Water Dimer Radical Cation Isomers 1 and 7.** The singly occupied molecular orbitals (SOMO) of the  $(\text{H}_2\text{O})_2^+$  isomers **1** and **7** are shown in Figure 6.

The hydrogen-bonded equilibrium structure **1** of the water dimer radical cation  $(\text{H}_2\text{O})_2^+ \tilde{X}^2\text{A} (C_1)$  in Group A has the following electron configuration



where [core] denotes the two lowest-lying core [O: 1s-like] orbitals 1a and 2a. The single electron occupying the 10a orbital “experiences” predominantly  $\text{O}_1$  oxygen 2p character. The hemibonded structure **7** of the water dimer radical cation  $(\text{H}_2\text{O})_2^+ {}^2\text{B} (C_2)$  has the following electron configuration



where the 5b orbital (SOMO) also has  $\text{O}_1$  oxygen 2p character. For this isomer there is the possibility of symmetry breaking of the ROHF reference wave function.<sup>71–74</sup> In particular, the SOMO may have a propensity to localize on either oxygen atom. We consider this problem in more detail when discussing the vibrational frequencies of isomer **7**.

**3. Charge Distributions of the Neutral Water Dimer and the Water Dimer Radical Cation Isomers 1 and 7.** Natural population analysis (NPA) of atomic populations<sup>75–77</sup> for the neutral water dimer and the water dimer radical cation isomers **1** and **7** are reported in Figure 7. To form the cation, one electron must be removed from the electron-rich  $\text{O}_1$  2p orbital in neutral water dimer. There are two possibilities for charge redistribution to prevent  $\text{O}_1$  from carrying a positive charge. The lowest energy isomer **1** results from atom  $\text{H}_4$  migrating toward atom  $\text{O}_2$  to form  $\text{H}_3\text{O}^+$ , and  $\text{OH}^\bullet$ , which are bound by a hydrogen bond. The other option is for the monomers to reorient and equally share the charge. This will lead to isomer **7**, which has  $C_2$  symmetry. The NPA results of isomer **1** and **7** with ROHF reference agree with those with UHF reference.

**C. Harmonic Vibrational Analyses: Comparison to Related Experiments.** The 12 harmonic vibrational frequencies for the different structures of  $(\text{H}_2\text{O})_2^+$  at the aug-cc-pVQZ CCSD(T) level of theory are presented in Table 2. The harmonic vibrational frequencies for the two minima **1** and **7** with the six different basis sets at the CCSD and CCSD(T) levels of theory are provided as Table 3 of Supporting Information, the IR intensities at the cc-pVTZ CCSD level of theory are also included.

Accompanying the formation of the water dimer, six additional low frequency vibrational motions are generated. Because of low energy barriers along those six vibrational modes, a number of stationary points have been located on the potential energy surface, specifically incorporating symmetry constraints for the dimer.

Among the five structures (**1–5**) in Group A ( $\text{H}_2\text{O}-\text{H}^+\cdots\text{OH}$  hydrogen-bonded system), isomer **1** is found to be the equilibrium structure, **2**, **3**, and **4** are transition states, and structure **5** is a second-order saddle point. The eigenvectors for the imaginary vibrational frequencies of structures **2** and **3** are associated with  $\text{O}_1\text{H}_3$  group rotations along the  $\text{O}_1\text{H}_4\text{O}_2$  axis. Structures **2** and **3** connect the two mirror images of isomer **1** in trans- and cis- conformation, respectively. The imaginary

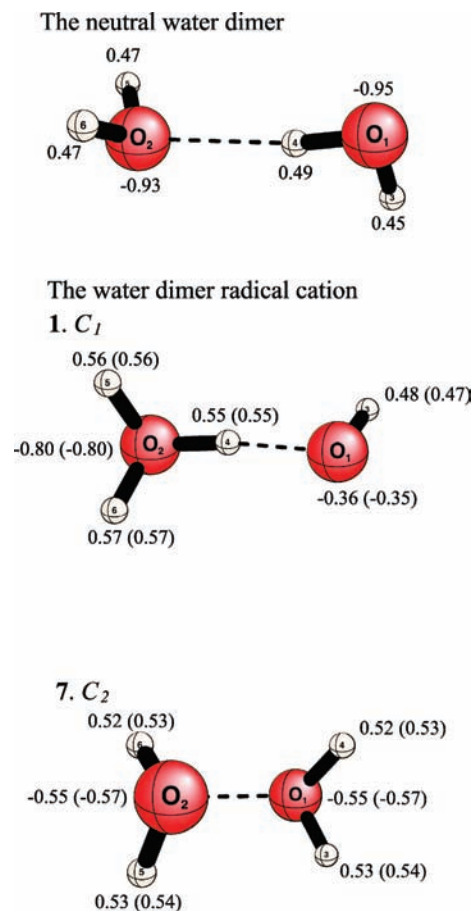


**Figure 7.** NPA atomic populations for the neutral water dimer and the water dimer radical cation isomers **1** and **7** with ROHF reference (values with UHF reference are in parentheses).

frequency of structure **4** may be attributed to the constraint on the planar conformation of the  $\text{H}_3\text{O}^+$  fragment, since the eigenvector of this frequency is the pyramidalization mode of  $\text{H}_3\text{O}^+$ , leading to **1**. There are two imaginary frequencies of structure **5**, and the corresponding eigenvectors are related to the tilting of the  $\text{O}_1\text{H}_3$  bond from linearity and the pyramidalization of the planar  $\text{H}_3\text{O}^+$  fragment.

Group B structure **6** ( $\text{H}_3\text{O}^+\cdots\text{OH}$ ) is found to be a transition state and structure **9** a second-order saddle point. The eigenvector corresponding to the imaginary frequency of structure **6** involves the rotation of the H atoms of the  $\text{H}_3\text{O}^+$  fragment along the  $\text{O}\cdots\text{O}$  axis to form a hydrogen-bonded structure. The two eigenvectors corresponding to imaginary frequencies for structure **9** are related to the rotation of the H atoms along the  $\text{O}\cdots\text{O}$  axis and the pyramidalization of the planar  $\text{H}_3\text{O}^+$  fragment.

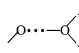
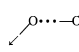
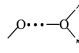
Among the seven structures in Group C (the  $[\text{H}_2\text{O}\cdots\text{H}_2\text{O}]^+$  hemibonded system), isomer **7** is found to be a minimum, **8**, **10**, and **11** are found to be transition states, and structures **12–14** are found to be higher-order saddle points. The normal mode with an imaginary frequency for structure **8** lowers the symmetry from  $C_{2h}$  (**8**) to  $C_2$  (**7**), while that for structure **11** lowers the symmetry from  $C_{2v}$  (**11**) to  $C_2$  (**7**). Structure **10** is the transition state for the isomerization reaction between **1** and **7**. The eigenvector of imaginary frequency ( $615i \text{ cm}^{-1}$ ) lowers the symmetry of **7** from  $C_2$  to  $C_1$  by shifting the  $\text{H}_4$  atom toward the  $\text{O}_2$  atom to form a hydrogen bond.

Among the 12 vibrational modes of all the water dimer radical cations, the four highest frequencies are associated with the four OH stretching motions. Structures **1–3** in Group A and structure

**TABLE 2: Harmonic Vibrational Frequencies (in  $\text{cm}^{-1}$ ) of the Neutral Water Dimer ( $\text{H}_2\text{O}$ )<sub>2</sub> and the Fourteen Stationary Points of Water Dimer Radical Cation ( $\text{H}_2\text{O}$ )<sub>2</sub><sup>+</sup> at the aug-cc-pVQZ CCSD(T) Level of Theory**

	$\omega_1$	$\omega_2$	$\omega_3$	$\omega_4$	$\omega_5$	$\omega_6$	$\omega_7$	$\omega_8$	$\omega_9$	$\omega_{10}$	$\omega_{11}$	$\omega_{12}$
H <sub>2</sub> O	3940	3831	1649									
H <sub>2</sub> O <sup>+</sup>	3440	3383	1474									
H <sub>3</sub> O <sup>+</sup>	3699	3699	3600	1699	1699	896						
OH	3738											
neutral	3931	3912	3825	3748	1671	1651	618	354	186	151	143	127
<b>1</b>	3780	3702	3666	2373	1719	1658	1050	617	503	400	360	98
<b>2</b>	3776	3700	3662	2364	1675	1651	1157	625	447	439	359	78 <i>i</i>
<b>3</b>	3787	3708	3668	2403	1670	1649	1111	579	454	452	357	158 <i>i</i>
<b>4</b>	3872	3769	3663	2254	1692	1568	784	618	396	375	148	521 <i>i</i>
<b>5</b>	3864	3764	3738	3033	1674	1621	584	475	334	330	476 <i>i</i>	620 <i>i</i>
<b>6</b>	3728	3720	3628	3588	1680	1655	1016	403	289	284	246	349 <i>i</i>
<b>7</b>	3713	3711	3638	3594	1611	1585	804	653	637	631	481	67
<b>8</b>	3709	3708	3637	3592	1621	1584	808	654	641	631	477	52 <i>i</i>
<b>9</b>	3841	3762	3728	3650	1609	1557	468	321	285	257	328 <i>i</i>	663 <i>i</i>
<b>10</b>	3815	3702	3575	3351	1610	1545	637	511	465	412	302	615 <i>i</i>
<b>11</b>	3865	3783	3337	3270	1685	1461	465	454	348	332	172	600 <i>i</i>
<b>12</b>	3908	3817	3472	3404	1679	1462	328	290	173	162 <i>i</i>	252 <i>i</i>	576 <i>i</i>
<b>13</b>	3884	3883	3710	3672	1497	1130	565	545	532	330 <i>i</i>	1096 <i>i</i>	1244 <i>i</i>
<b>14</b>	3869	3816	3756	3558	1573	568	523	353	81	383 <i>i</i>	603 <i>i</i>	2042 <i>i</i>

**TABLE 3: Comparison of the Present Water Dimer Radical Cation Vibrational Frequencies (in  $\text{cm}^{-1}$ ) with Those of Gardener, Johnson, and McCoy<sup>27a</sup>**

	$(\text{H}_2\text{O})_2^+$		$(\text{H}_2\text{O})_2^+ \cdot \text{Ar}$		$(\text{H}_2\text{O})_2^+ \cdot \text{Ar}_2$	
	This work CCSD(T) aug-cc-pVQZ	UMP2 aug-cc-pVDZ	Experiment	UMP2 aug-cc-pVDZ	Experiment	UMP2 aug-cc-pVDZ
$\nu_p$	98	99		89		89
$\nu_{\text{bend}}$	1658	1643	1543	1635	1601	1644
$\nu_{\text{sp(L)}}$	1719	1696		1699		1697
$\nu_{\text{sp(U)}}$			1863		1916	
			1975	2475	2021	2593
			2078		2155	
$\nu_{\text{OH}}^{\text{Ar}}$ or $\nu_{\text{OH}}^{\text{sym}}$	 3702	3660	3392	3450	3392	3544
$\nu_{\text{OH}}$	 3666	3678	3511	3685	3499	3691
$\nu_{\text{OH}}^{\text{Ar}}$ or $\nu_{\text{OH}}^{\text{sym}}$	 3780	3758	3591	3732	3408	3614

<sup>a</sup> The latter authors also report results for  $(\text{H}_2\text{O})_2^+ \cdot \text{Ar}_n$  ( $n = 0, 1$  and  $2$ ). The theoretical frequencies are harmonic, while the experimental frequencies are fundamentals.

**6** in Group B all have three HOH bending modes (the next highest frequencies) related to the  $\text{H}_3\text{O}^+$  moiety of the cation, the third one corresponds to the pyramidalization motion including all three OH bonds. While structures **4** and **5** in Group A and structure **9** in Group B present two HOH bending and one out-of-plane motions. The seven structures (**7**, **8**, **10–14**) in Group C show two HOH bending motions from each of the  $\text{H}_2\text{O}$  and  $\text{H}_2\text{O}^+$  fragments, respectively.

For the  $(\text{H}_2\text{O})_2^+$  isomer **1** the antisymmetric ( $\omega_1 = 3780 \text{ cm}^{-1}$ ), and symmetric ( $\omega_2 = 3702 \text{ cm}^{-1}$ ) stretches of the  $\text{H}_3\text{O}^+$  fragment are higher than those for the isolated  $\text{H}_3\text{O}^+$  molecule, whereas they are lower than those for the neutral water dimer. The third OH stretch ( $\omega_3 = 3666 \text{ cm}^{-1}$ , OH radical moiety) is lower than that ( $3738 \text{ cm}^{-1}$ ) of the isolated OH radical, due to the longer OH bond distance. The shared  $\text{O}_2\text{H}_4$  ( $\omega_4 = 2373 \text{ cm}^{-1}$ ) stretching feature of isomer **1** shows the lowest OH stretching frequency, reflecting the longest OH separation ( $1.048 \text{ \AA}$  hydrogen-bonded) in the molecule.

Very recently, Gardener, Johnson, and McCoy (GJM) trapped the nascent  $[\text{H}_3\text{O}^+ \cdot \text{OH}]$  exit channel intermediate via Ar-

mediated ionization of the neutral water dimer. They characterized the nature of the ion-radical complex using vibrational predissociation spectroscopy of the Ar-tagged species.<sup>27</sup> Gardener reported the spectra of  $\text{H}_4\text{O}_2^+ \cdot \text{Ar}_n$ , for one or two argon atoms bound to the  $\text{H}_3\text{O}^+$  end of the  $[\text{H}_3\text{O}^+ \cdot \text{OH}]$  complex. The Johnson–McCoy collaboration also computed the harmonic vibrational frequencies of the equilibrium structure at the UMP2/aug-cc-pVDZ level. There are considerable differences between the experimental fundamental and theoretical harmonic frequencies, presumably largely due to anharmonic effects. The comparison of vibrational frequencies (in  $\text{cm}^{-1}$ ) from Gardener, Johnson, and McCoy and our research is shown in Table 3.

For both the one and two argon-bound  $[\text{H}_3\text{O}^+ \cdot \text{OH}]$  spectra, there are three peaks corresponding to OH stretching, in the  $3200\text{--}3600 \text{ cm}^{-1}$  region. The experimental asymmetric OH stretches are at  $3408$  and  $3591 \text{ cm}^{-1}$ , respectively, for the  $(\text{H}_2\text{O})_2^+ \cdot \text{Ar}_2$  and  $(\text{H}_2\text{O})_2^+ \cdot \text{Ar}$  complexes. This large difference between the above two frequencies reflects the strong interaction of the radical cation with argon. For isomer **1**, from our research the harmonic asymmetric OH stretch ( $\omega_1$ ) of the  $\text{H}_3\text{O}^+$  fragment

at the aug-cc-pVQZ/CCSD(T) level is  $3780\text{ cm}^{-1}$ , necessarily higher than the observed fundamentals, but in good agreement with the aug-cc-pVDZ/UMP2 harmonic frequencies  $3758\text{ cm}^{-1}$  for the no Ar-attached  $(\text{H}_2\text{O})_2^+$  [ $3732$  and  $3614\text{ cm}^{-1}$  for  $(\text{H}_2\text{O})_2^+\cdot\text{Ar}_n$  ( $n = 1$  and  $2$ )]. The symmetric stretch harmonic frequency ( $\omega_2 = 3702\text{ cm}^{-1}$ ) of the  $\text{H}_3\text{O}^+$  fragment at the aug-cc-pVQZ/CCSD(T) level is also in reasonable agreement with the aug-cc-pVDZ/UMP2 result at  $3660\text{ cm}^{-1}$  [ $3450$  and  $3544\text{ cm}^{-1}$  for  $(\text{H}_2\text{O})_2^+\cdot\text{Ar}$  and  $(\text{H}_2\text{O})_2^+\cdot\text{Ar}_2$ ]. The analogous experimental features for  $(\text{H}_2\text{O})_2^+\cdot\text{Ar}$  and  $(\text{H}_2\text{O})_2^+\cdot\text{Ar}_2$  lie at  $3392$  and  $3392\text{ cm}^{-1}$ . The third high-frequency peak corresponding to the OH stretch of the OH radical moiety, is observed at  $3511$  and  $3499\text{ cm}^{-1}$  for  $(\text{H}_2\text{O})_2^+\cdot\text{Ar}$  and  $(\text{H}_2\text{O})_2^+\cdot\text{Ar}_2$ . Our result ( $\omega_3 = 3666\text{ cm}^{-1}$ ) is in good agreement with GJM's aug-cc-pVDZ/UMP2 harmonic frequency at  $3678\text{ cm}^{-1}$  [ $3685$  and  $3691\text{ cm}^{-1}$  for  $(\text{H}_2\text{O})_2^+\cdot\text{Ar}$  and  $(\text{H}_2\text{O})_2^+\cdot\text{Ar}_2$ ].

With the introduction of the first and second argon atoms, there is an approximately  $100\text{ cm}^{-1}$  blue shift in the shared  $\text{O}\cdots\text{H}$  stretch region ( $1800\text{--}2000\text{ cm}^{-1}$ ) of the spectra. This experimental shift is opposite in direction to the shift in the exterior OH stretch [the shared  $\text{O}\cdots\text{H}$  stretching frequency in  $(\text{H}_2\text{O})_2^+\cdot\text{Ar}_2$  is higher than that in  $(\text{H}_2\text{O})_2^+\cdot\text{Ar}$ ]. We predict this  $\text{O}\cdots\text{H}$  stretching mode to be at  $2373\text{ cm}^{-1}$  for the Ar-free  $(\text{H}_2\text{O})_2^+$  from the aug-cc-pVQZ/CCSD(T) level,  $53\text{ cm}^{-1}$  higher than the aug-cc-pVDZ/UMP2 result for  $(\text{H}_2\text{O})_2^+$  ( $2320\text{ cm}^{-1}$ ), but lower than the aug-cc-pVDZ/UMP2 results for  $(\text{H}_2\text{O})_2^+\cdot\text{Ar}$  and  $(\text{H}_2\text{O})_2^+\cdot\text{Ar}_2$  ( $2475$  and  $2593\text{ cm}^{-1}$ ). GJM states that the fundamental in the intracomplex proton-transfer mode appears as a triplet rather than as a single peak. They tentatively assigned this feature to reflect the hindered OH rotational structure of the hydroxyl moiety, built off the fundamental associated with the bridging proton vibration parallel to the  $\text{O}\cdots\text{O}$  axis. In our research, among the seven proton-transferred structures in Group A (**1**–**5**) and B (**6** and **9**), four structures (**2**–**4** and **6**) were found to be transition states, which may be connected to the global minimum **1**. Specifically, three transition states (**2**–**4**) lie no more than  $1.44\text{ kcal mol}^{-1}$  ( $0.60\text{ kcal mol}^{-1}$  with ZPVE corrections) above **1**. Therefore, these low barrier (low imaginary frequency) motions might produce such complicated triplet splitting spectra for the Ar-tagged  $(\text{H}_2\text{O})_2^+$  complexes, as also suggested by GJM.

In the  $(\text{H}_2\text{O})_2^+$  vibrational spectrum, there is also a water bend region ( $1500\text{--}1600\text{ cm}^{-1}$ ), which corresponds to the intermolecular (HOH) bend of the hydronium constituent or the off-axis displacement of the shared proton. We predict the corresponding harmonic frequencies at  $1719$  and  $1658\text{ cm}^{-1}$  with aug-cc-pVQZ/CCSD(T) method; while at aug-cc-pVDZ/UMP2 level of theory, GJM computed the two harmonic frequencies at  $1696$  and  $1643\text{ cm}^{-1}$  for the Ar-free  $(\text{H}_2\text{O})_2^+$ .

The four OH stretching frequencies of the hemibonded structure **7** fall between the two OH stretching frequencies of the neutral water monomer and those of the water monomer cation, due to the intermediate OH bond distances. The two HOH bending frequencies of **7** again fall between the bending frequencies of  $\text{H}_2\text{O}$  and  $\text{H}_3\text{O}^+$ , reflecting the intermediate HOH bond angles. An orbital stability analysis of the ROHF wave function used in the harmonic vibrational frequencies calculation reveals that there is one instability connected to the mixing of SOMO and SOMO–1. This leads to localization of the SOMO and SOMO–1 as well as charge localization on the two equivalent oxygen atoms. To examine the effect of this orbital instability on the frequencies, we have reoptimized the geometry and recomputed vibrational frequencies for isomer **7** at the UHF-UCCSD level using the cc-pVTZ basis set. At this level of

theory, the UHF reference does not show any orbital instability and the relative energy and frequencies are in very good agreement with the ROHF-UCCSD results. The UHF-UCCSD relative energy deviates from the ROHF-UCCSD value by  $0.44\text{ kcal mol}^{-1}$ . The largest shift in the vibrational frequencies is found for the HOH wagging (B) mode ( $676\text{ cm}^{-1}$  for UHF-UCCSD and  $660\text{ cm}^{-1}$  for ROHF-UCCSD). Consequently, we believe that for the highly correlated wave functions adopted in this work, there are no significant effects from the instability of the ROHF reference on the energetics and the physical properties of water dimer cation. Table 2 reveals that structures **13** and **14** possess imaginary vibrational frequencies with alarming high magnitudes. To confirm that these are not artifacts of symmetry breaking, we performed stability analyses on the ROHF reference wave functions, confirming their stability. UHF-UCCSD theory yields similar vibrational frequency results.

**D. Energetics.** The schematic potential energy surface [CCSD(T) level with aug-cc-pVQZ basis] for proton-transfer and dissociation processes for the hemibonded isomer **7** and the hydrogen-bonded isomer **1** is shown in Figure 8. The complete list of electronic energies for all stationary points is provided in the Supporting Information.

Relative energies (in  $\text{kcal mol}^{-1}$ ) of all the stationary points of  $(\text{H}_2\text{O})_2^+$  with respect to the global minimum of water dimer radical cation (isomer **1**) at the CCSD and CCSD(T) levels with the cc-pVQZ and aug-cc-pVQZ basis sets are presented in Table 4. The energy differences between these 14 stationary points are in the range  $0.05\text{--}45.5\text{ kcal mol}^{-1}$  with the aug-cc-pVQZ CCSD method, and  $0.05\text{--}44.6\text{ kcal mol}^{-1}$  with the aug-cc-pVQZ CCSD(T) method.

At our highest level of theory, aug-cc-pVQZ CCSD(T), the global minimum of the water dimer radical cation isomer **1** (in group A, hydrogen-bonded system) is predicted to be  $7.1\text{ kcal mol}^{-1}$  ( $8.8\text{ kcal mol}^{-1}$  with the zero-point vibrational energy, ZPVE) lower in energy than isomer **7** in Group C (hemibonded system). Gill and Radom computed this energy difference to be  $8.9\text{ kcal mol}^{-1}$  at the MP4/6-311G(MC)\*\*//MP2/6-31G\* level of theory,<sup>56</sup> while Sodupe and Bertran determined the energy difference to be  $9.8\text{ kcal mol}^{-1}$  at the MCPHF/TZ2P++//MP2/TZ2P++ level of theory,<sup>57</sup> and  $7.7\text{ kcal mol}^{-1}$  using DFT.<sup>78</sup> Quite recently, Pieniazek et al. computed the energy difference of the two isomers to be  $8.2\text{ kcal mol}^{-1}$  at the CCSD(T)/6-311++G\*\*//EOM-IP-CCSD/6-311++G\*\* level of theory.<sup>1</sup> The energy barrier for the forward (**1**  $\rightarrow$  **10**  $\rightarrow$  **7**) reaction between the two isomers is here predicted to be  $15.1$  (also  $15.1$  with ZPVE correction)  $\text{kcal mol}^{-1}$  at the aug-cc-pVQZ CCSD(T) level of theory. For the reverse (**7**  $\rightarrow$  **10**  $\rightarrow$  **1**) reaction the barrier is predicted to be  $8.1$  ( $7.4$  with ZPVE correction)  $\text{kcal mol}^{-1}$ .

The potential energy surface that connects the hydrogen-bonded isomers **1**, **2** and **3** is extremely flat. The transition states **2** (*trans-C<sub>s</sub>*) lies  $0.05\text{ kcal mol}^{-1}$ , and **3** (*cis-C<sub>s</sub>*) is  $0.73\text{ kcal mol}^{-1}$  higher in energy than the global minimum **1** at the aug-cc-pVQZ CCSD(T) level. With ZPVE correction, **2** (*trans-C<sub>s</sub>*) is  $0.06\text{ kcal mol}^{-1}$  lower in energy and **3** (*cis-C<sub>s</sub>*) is  $0.60\text{ kcal mol}^{-1}$  higher in energy at the same level of theory. Since the imaginary vibrational frequencies of **2** and **3** are only  $78i$  and  $1586\text{ cm}^{-1}$  ( $0.22$  and  $0.45\text{ kcal mol}^{-1}$ ), such small PES energy differences cannot hinder essentially free  $\text{O}_1\text{H}_3$  rotation about the  $\text{O}_1\text{H}_4\text{O}_2$  axis.

The neutral water dimer  $(\text{H}_2\text{O})_2$  (<sup>1</sup>A' state with *C<sub>s</sub>* symmetry) obviously has a lower energy than two separated water molecules. This is due to hydrogen bonding, yielding a destabilization of the HOMO orbital of the proton donor and



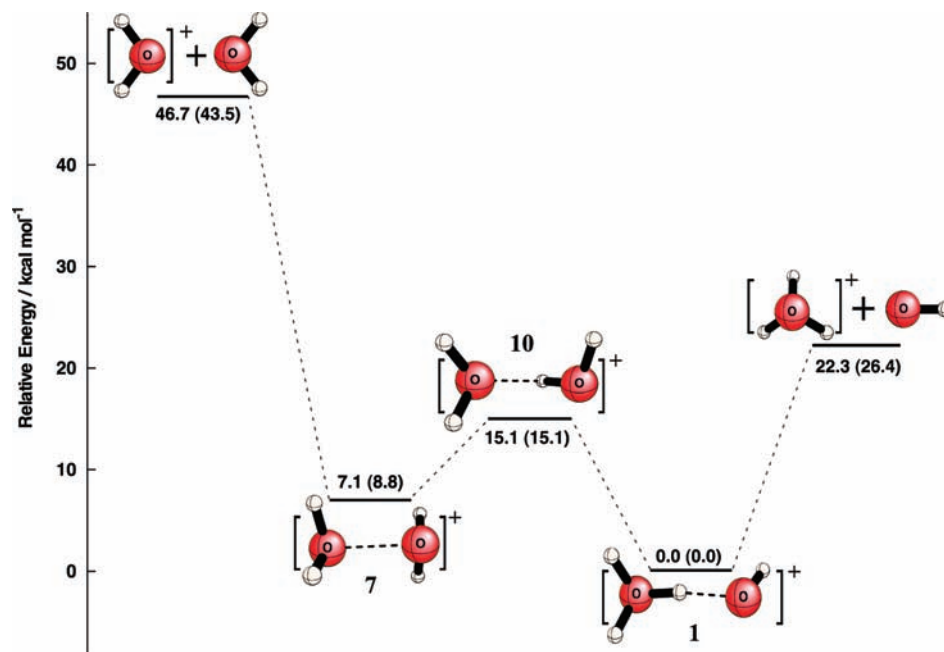


**Figure 8.** Schematic potential energy surface (in kcal mol<sup>-1</sup>, ZPVE corrected values in parentheses) showing proton-transfer and dissociation processes for the hemibonded and hydrogen-bonded water dimer radical cation structures **1**, **7**, and **10** at the aug-cc-pVQZ CCSD(T) level of theory.

**TABLE 4: Relative Energies (in kcal mol<sup>-1</sup>, ZPVE Corrected Values in Parentheses) of the 14 Stationary Points of the Water Dimer Radical Cation (H<sub>2</sub>O)<sub>2</sub><sup>+</sup> with Respect to Isomer 1 at the CCSD and CCSD(T) Levels**

	CCSD/ cc-pVQZ	CCSD/ aug-cc-pVQZ	CCSD(T)/ cc-pVQZ	CCSD(T)/ aug-cc-pVQZ
<b>1</b>	0.00(0.00)	0.00(0.00)	0.00(0.00)	0.00(0.00)
<b>2</b>	0.04(-0.07)	0.05(-0.06)	0.04(-0.08)	0.05(-0.06)
<b>3</b>	0.74(0.58)	0.71(0.58)	0.75(0.60)	0.73(0.60)
<b>4</b>	1.37(0.26)	1.39(0.27)	1.42(0.29)	1.44(0.31)
<b>5</b>	4.19	4.18	5.29	5.24
<b>6</b>	6.30	6.25	6.75	6.67
<b>7</b>	10.15(12.01)	9.90(11.74)	7.41(9.14)	7.09(8.80)
<b>8</b>	10.15(11.94)	9.90(11.69)	7.41(9.05)	7.10(8.72)
<b>9</b>	8.68	8.62	9.26	9.17
<b>10</b>	16.81(16.99)	16.65(16.49)	15.37(15.41)	15.14(15.14)
<b>11</b>	20.34(19.35)	20.27(19.23)	20.27(19.25)	20.18(19.10)
<b>12</b>	36.59	36.11	36.85	36.29
<b>13</b>	36.75	36.38	34.71	34.24
<b>14</b>	45.89	45.52	45.09	44.63

stabilization of the HOMO orbital of the proton acceptor. Removing one electron from the neutral water dimer forms a <sup>2</sup>A'' vertical ionized state, and subsequent geometrical relaxation of the <sup>2</sup>A'' ionic state leads to the structure with the hydrogen atom involved in the hydrogen bonding transferred to the water acceptor molecule.

The binding energies of (H<sub>2</sub>O)<sub>2</sub><sup>+</sup> with respect to isolated H<sub>3</sub>O<sup>+</sup> plus OH<sup>•</sup> and isolated H<sub>2</sub>O<sup>+</sup> plus H<sub>2</sub>O are presented in Table 5. With the aug-cc-pVQZ basis set, the binding energies for the 14 stationary points fall in the range 0.9–46.4 kcal mol<sup>-1</sup> (CCSD), 2.1–46.7 kcal mol<sup>-1</sup> [CCSD(T)] compared to (H<sub>2</sub>O<sup>+</sup> + H<sub>2</sub>O) fragments. Therefore, all these stationary points of the water dimer radical cation are at least somewhat more favorable than the isolated H<sub>2</sub>O<sup>+</sup> and H<sub>2</sub>O molecules. The total energy of isolated OH radical and H<sub>3</sub>O<sup>+</sup> molecules is lower than the isolated H<sub>2</sub>O and H<sub>2</sub>O<sup>+</sup> molecules [24.8 kcal mol<sup>-1</sup> lower at CCSD and 24.4 kcal mol<sup>-1</sup> lower at CCSD(T)]. The binding energies for all these stationary points with respect to the fragments (H<sub>3</sub>O<sup>+</sup> + OH<sup>•</sup>) are determined to be -23.9 to 21.7

kcal mol<sup>-1</sup> (CCSD), and -22.3 to 22.3 kcal mol<sup>-1</sup> [CCSD(T)]. The water dimer radical cation structures **12**, **13**, and **14** have higher energies than the isolated H<sub>3</sub>O<sup>+</sup> and OH<sup>•</sup> molecules. The binding energies in Table 5 confirm that the dissociation of (H<sub>2</sub>O)<sub>2</sub><sup>+</sup> is more likely going through the oxonium channel (H<sub>3</sub>O<sup>+</sup> + OH<sup>•</sup>) rather than the water channel (H<sub>2</sub>O<sup>+</sup> + H<sub>2</sub>O), especially considering the structure of **1**.

Relative energies (in eV) of all the stationary points of (H<sub>2</sub>O)<sub>2</sub><sup>+</sup> with respect to the ground electronic state of the neutral water dimer  $\tilde{X}^1A'$  at the CCSD and CCSD(T) levels with the cc-pVTZ, cc-pVQZ, aug-cc-pVTZ and aug-cc-pVQZ basis sets are displayed in Table 6. With the aug-cc-pVQZ basis set, the energy differences range 10.74–12.71 eV at the CCSD level and 10.84–12.77 eV at CCSD(T) level. Including the zero-point vibrational energy (ZPVE) correction, the energy differences are 10.71–12.57 eV and 10.81–12.63 eV at the CCSD and CCSD(T) levels of theory with the same basis set, respectively.

The adiabatic ionization energy of the water dimer from our study is 10.8 eV (also 10.8 eV with ZPVE correction) using the aug-cc-pVQZ CCSD(T) method, which is in excellent agreement with the experimental adiabatic (threshold) ionization energy of 10.8–10.9 eV. The theoretical <sup>2</sup>A'' state vertical ionization energy of 11.9 eV at the same level of theory is in reasonable agreement with the experimental value of 12.1 ± 0.1 eV.<sup>53</sup> This large difference (1.1 eV) between the vertical and adiabatic ionization energies is due to the tremendous change in the equilibrium geometries between the neutral water dimer and the water dimer radical cation. The theoretical vertical ionization energy for the <sup>2</sup>A' state is 13.2 eV (at the same level of theory), where the experimental value is 13.2 ± 0.2 eV.<sup>53</sup> This IP is significantly higher than the first ionization energy, reflecting the considerable difference in the 2a'' (-0.48 hartree) and 8a' (-0.53 hartree) orbital energies for the neutral water dimer.

#### IV. Conclusions

Ab initio coupled-cluster electronic structure theory has been employed in order to investigate the water dimer radical cation

**TABLE 5: Relative Energies (in kcal mol<sup>-1</sup>, ZPVE Corrected Values in Parentheses) of the 14 Stationary Points of Water Dimer Radical Cation (H<sub>2</sub>O)<sub>2</sub><sup>+</sup> with Respect to the Water (H<sub>2</sub>O<sup>+</sup> + H<sub>2</sub>O) and the Oxonium (H<sub>3</sub>O<sup>+</sup>+OH) Dissociation Channels at the CCSD and CCSD(T) Levels Using the aug-cc-pVQZ Basis Set**

structure	(H <sub>2</sub> O <sup>+</sup> -H <sub>2</sub> O)		(H <sub>3</sub> O <sup>+</sup> -OH)		
	CCSD/aug-cc-pVQZ	CCSD(T)/aug-cc-pVQZ	CCSD/aug-cc-pVQZ	CCSD(T)/aug-cc-pVQZ	
1	C <sub>1</sub>	46.43(43.20)	46.68(43.52)	21.66(25.69)	22.31(26.38)
2	trans-C <sub>s</sub>	46.38(43.26)	46.64(43.58)	21.61(25.75)	22.27(26.43)
3	cis-C <sub>s</sub>	45.71(42.62)	45.96(42.92)	20.94(25.11)	21.59(25.77)
4	planar C <sub>s</sub>	45.03(42.93)	45.24(43.21)	20.26(25.42)	20.88(26.06)
5	planar C <sub>2v</sub>	42.25	41.44	17.48	17.07
6	C <sub>s</sub>	40.18	40.01	15.41	15.64
7	C <sub>2</sub>	36.53(31.46)	39.59(34.72)	11.76(13.95)	15.22(17.57)
8	C <sub>2h</sub>	36.53(31.51)	39.59(34.80)	11.76(14.00)	15.22(17.65)
9	planar C <sub>2v</sub>	37.81	37.51	13.04	13.14
10	C <sub>1</sub>	29.78(26.71)	31.54(28.39)	5.01(9.20)	7.17(11.24)
11	cis-bifurcated C <sub>2v</sub>	26.16(23.97)	26.50(24.42)	1.39(6.46)	2.13(7.27)
12	trans-bifurcated C <sub>2v</sub>	10.31	10.39	-14.45	-13.98
13	D <sub>2h</sub>	10.05	12.45	-14.72	-11.92
14	planar C <sub>2v</sub>	0.90	2.05	-23.87	-22.32

**TABLE 6: Relative Energies (in eV, ZPVE Corrected Values in Parentheses) of the <sup>2</sup>A'' and <sup>2</sup>A' Vertical Ionized States of the Neutral Water Dimer and the Fourteen Stationary Points of Water Dimer Radical Cation (H<sub>2</sub>O)<sub>2</sub><sup>+</sup> with Respect to the Ground Electronic State of the Neutral Water Dimer at the CCSD and CCSD(T) Levels<sup>a</sup>**

	CCSD/ cc-pVQZ	CCSD/ aug-cc-pVQZ	CCSD(T)/ cc-pVQZ	CCSD(T)/ aug-cc-pVQZ
(H <sub>2</sub> O) <sub>2</sub>	0.00(0.00)	0.00(0.00)	0.00(0.00)	0.00(0.00)
<sup>2</sup> A'	13.22	13.28	13.16	13.21
<sup>2</sup> A''	11.71	11.77	11.78	11.85
1	10.66(10.63)	10.74(10.72)	10.74(10.72)	10.84(10.81)
2	10.66	10.74	10.75	10.84
3	10.69	10.77	10.78	10.87
4	10.72	10.80	10.81	10.90
5	10.84	10.92	10.97	11.06
6	10.93	11.01	11.04	11.13
7	11.10(11.15)	11.17(11.23)	11.07(11.11)	11.14(11.19)
8	11.10	11.17	11.07	11.14
9	11.03	11.11	11.15	11.23
10	11.39	11.46	11.41	11.49
11	11.54	11.62	11.62	11.71
12	12.24	12.30	12.34	12.41
13	12.25	12.32	12.25	12.32
14	12.65	12.71	12.70	12.77

<sup>a</sup> Experimental value = 10.8–10.9 eV from ref 14.

molecules. Fourteen stationary points have been located on the electronic doublet ground state PES. Based on the harmonic vibrational frequency analyses, two minima (*0i*) with C<sub>1</sub> and C<sub>2</sub> symmetries, 7 transition states (*1i*), and 5 higher order saddle points (*2i* or more) have been characterized. Stationary point geometries and energetics are very sensitive to basis sets and levels of sophistication. At our highest level of theory, aug-cc-pVQZ CCSD(T), the energy differences among all these radical cation stationary points fall in the range of 44.6 kcal mol<sup>-1</sup>. The global minimum of the water dimer radical cation has been confirmed to be a hydrogen-bonded system with C<sub>1</sub> point group symmetry **1**, which lies 7.1 (8.8 with ZPVE correction) kcal mol<sup>-1</sup> lower in energy than the hemibonded isomer **7** with C<sub>2</sub> point group symmetry. The dissociation energy of isomer **1** via the oxonium channel [H<sub>2</sub>O-H<sup>+</sup>...OH → H<sub>3</sub>O<sup>+</sup> + OH•] has been predicted to be 22.3 (26.4 with ZPVE correction) kcal mol<sup>-1</sup>. The dissociation energy of isomer **7** via the water channel [(H<sub>2</sub>O)<sub>2</sub><sup>+</sup> → H<sub>2</sub>O<sup>+</sup> + H<sub>2</sub>O] is predicted to be 39.6 (34.7 with ZPVE correction) kcal mol<sup>-1</sup>. The energy barrier for the forward (**1** → **10** → **7**) isomerization reaction between the two isomers

has been determined to be 15.1 (also 15.1 with ZPVE correction) kcal mol<sup>-1</sup> at the aug-cc-pVQZ CCSD(T) level of theory. Therefore, the dissociation of the water dimer cation is likely to occur via the oxonium channel.

**Acknowledgment.** The authors would like to thank Dr. Justin M. Turney and Mr. Jeremiah Wilke for insightful discussions and technical expertise. This research was funded by the Department of Energy, Basic Energy Sciences, Division of Chemical Sciences, Fundamental Interactions Team. This research used the resources of the National Energy Research Scientific Computing Center (NERSC), supported by the Office of Science of the U.S. Department of Energy under Contract No. DE-AC02-05CH11231.

**Supporting Information Available:** Optimized molecular geometries, total electronic energies, and harmonic vibrational frequencies of the water dimer radical cation at various levels of theory.

This material is available free of charge via the Internet at <http://pubs.acs.org>.

## References and Notes

- Pieniazek, P. A.; VandeVondele, J.; Jungwirth, P.; Krylov, A. I.; Bradforth, S. E. *J. Phys. Chem. A* **2008**, *112*, 6159.
- Pieniazek, P. A.; Sundstrom, E. J.; Bradforth, S. E.; Krylov, A. I. *J. Phys. Chem.* **2009**, *113*, 4423.
- Liu, K.; Cuzan, J. D.; Saykally, R. J. *Science* **1996**, *271*, 929.
- Castleman, A. W. J.; Bowen, K. H. J. *J. Phys. Chem.* **1996**, *100*, 12911.
- Barnett, R. N.; Landman, U.; Cleveland, C. L. *J. Chem. Phys.* **1988**, *88*, 4421.
- Barnett, R. N.; Landman, U.; Cleveland, C. L. *J. Chem. Phys.* **1988**, *88*, 4429.
- Novakovskaya, Y. V.; Stepanov, N. F. *J. Phys. Chem.* **1999**, *103*, 3285.
- Su, Z.; Buhl, M.; Zhou, W. *J. Am. Chem. Soc.* **2009**, *131*, 8697.
- Kaukonen, H. P.; Barnett, R. N.; Landman, U. *J. Chem. Phys.* **1992**, *97*, 1365.
- Klots, C. E.; Compton, R. N. *J. Chem. Phys.* **1978**, *69*, 1644.
- Shinohara, H.; Nishi, N.; Washida, N. *J. Chem. Phys.* **1986**, *84*, 5561.
- Ng, C. Y.; Trevor, D. J.; Tiedemann, P. W.; Ceyer, S. T.; Kronebusch, P. L.; Mahan, B. H.; Lee, Y. T. *J. Chem. Phys.* **1977**, *67*, 4235.
- Haberland, H.; Langosch, H. *Z. Phys. D* **1986**, *2*, 243.
- DeVisser, S. P.; DeKoning, L. J.; Nibbering, N. M. M. *J. Phys. Chem.* **1995**, *99*, 15444.
- Castleman, A. W. J. *Springer Ser. Chem. Phys.* **1994**, *56*, 77.
- Angel, L.; Stace, A. J. *Chem. Phys. Lett.* **2001**, *345*, 277.

- (17) Yamaguchi, S.; Kudoh, S.; Kawai, Y.; Okada, Y.; Orii, T.; Takeuchi, K. *Chem. Phys. Lett.* **2003**, *377*, 37.
- (18) Golubeva, A. A.; Pieniazek, P. A.; Krylov, A. I. *J. Chem. Phys.* **2009**, *130*, 124113.
- (19) McCoy, A. B.; Huang, X.; Carter, S.; Bowman, J. M. *J. Chem. Phys.* **2005**, *123*, 064317.
- (20) McCunn, L. R.; Roscioli, J. R.; Johnson, M. A.; McCoy, A. B. *J. Phys. Chem. B* **2008**, *112*, 321.
- (21) McCoy, A. B. *Int. Rev. Phys. Chem.* **2006**, *25*, 77.
- (22) Crofton, M. W.; Price, J. M.; Lee, Y. T. *Springer Ser. Chem. Phys.* **1994**, *56*, 44.
- (23) Stace, A. J. *Phys. Rev. Lett.* **1988**, *61*, 306.
- (24) Stace, A. J. *Chem. Phys. Lett.* **1990**, *174*, 103.
- (25) Buck, U.; Winter, M. Z. *Phys. D* **1994**, *31*, 291.
- (26) Barnett, R. N.; Landman, U. *J. Phys. Chem.* **1995**, *99*, 17305.
- (27) Gardenier, G. H.; Johnson, M. A.; McCoy, A. B. *J. Phys. Chem.* **2009**, *113*, 4772.
- (28) Schulz, C. P.; Hertel, J. V. *Springer Ser. Chem. Phys.* **1994**, *56*, 7.
- (29) Barnett, R. N.; Landman, U. *Phys. Rev. Lett.* **1993**, *70*, 1775.
- (30) Hammer, N. I.; Diken, E. G.; Roscioli, J. R.; Johnson, M. A.; Myshakin, E. M.; Jordan, K. D.; McCoy, A. B.; Huang, X.; Bowman, J. M.; Carter, S. *J. Chem. Phys.* **2005**, *122*, 244301.
- (31) Frisch, M. J.; Del Bene, J. E.; Binkley, J. S.; Schaefer, H. F. *J. Chem. Phys.* **1986**, *84*, 2279.
- (32) Barnett, R. N.; Cheng, H. P.; Hakkinen, H.; Landman, U. *J. Phys. Chem.* **1995**, *99*, 7731.
- (33) Valeev, E. F.; Schaefer, H. F. *J. Chem. Phys.* **1998**, *108*, 7197.
- (34) Tomoda, S.; Achiba, Y.; Kimura, K. *Chem. Phys. Lett.* **1982**, *87*, 197.
- (35) Dong, F.; Heinbuch, S.; Rocca, J. J.; Bernstein, E. R. *J. Chem. Phys.* **2006**, *124*, 224319.
- (36) Bowen, K. H.; Eaton, J. G. *The Structure of Small Molecules and Ions*. Naaman, R., Voger, Z., Eds.; Plenum Press: New York, 1988; p 147.
- (37) Coe, J. V.; Lee, G. H.; Eaton, J. G.; Arnold, S. T.; Sarkas, H. W.; Bowen, K. H.; Ludewigt, C.; Haberland, H.; Worsnop, D. R. *J. Chem. Phys.* **1990**, *92*, 3980.
- (38) Lee, G. H.; Arnold, S. T.; Eaton, J. G.; Sarkas, H. W.; Bowen, K. H.; Ludewigt, C.; Haberland, H. *Z. Phys. D* **1991**, *20*, 9.
- (39) Desfrancois, C.; Khelifa, N.; Schermann, J. P.; Eaton, J. G.; Bowen, K. H. *J. Chem. Phys.* **1991**, *95*, 7760.
- (40) Barnett, R. N.; Landman, U.; Cleveland, C. L.; Jortner, J. *J. Chem. Phys.* **1988**, *88*, 4429.
- (41) Jordan, K. D. *Science* **2004**, *306*, 618.
- (42) Bragg, A. E.; Verlet, J. R. R.; Kammrath, A.; Cheshnovsky, O.; Neumark, D. M. *Science* **2004**, *306*, 669.
- (43) Ayotte, P.; Johnson, M. A. *J. Chem. Phys.* **1997**, *106*, 811.
- (44) Bailey, A. D.; Narcisi, R. S. *J. Geophys. Res.* **1965**, *70*, 3687.
- (45) Wei, S.; Shi, Z.; Castleman, A. W. *J. Chem. Phys.* **1991**, *94*, 3268.
- (46) Tomoda, S.; Kimura, K. *Chem. Phys.* **1983**, *82*, 215.
- (47) Barnett, R. N.; Landman, U. *J. Phys. Chem. A* **1997**, *101*, 164.
- (48) Tschumper, G. S.; Leininger, M. L.; Hoffman, B. C.; Valeev, E. F.; Schaefer, H. F.; Quack, M. *J. Chem. Phys.* **2002**, *116*, 690.
- (49) Tomoda, S.; Kimura, K. *Chem. Phys. Lett.* **1984**, *111*, 434.
- (50) Tachikawa, H. *J. Phys. Chem.* **2002**, *106*, 6159.
- (51) Gurtubay, I. G.; Drummond, N. D.; Towler, M. D.; Needs, R. J. *J. Chem. Phys.* **2006**, *124*, 24318.
- (52) Smith, B. J.; Swanton, D. J.; Pople, J. A.; Schaefer, H. F.; Radom, L. *J. Chem. Phys.* **1990**, *92*, 1240.
- (53) Sato, K.; Tomoda, S.; Kimura, K.; Iwata, S. *Chem. Phys. Lett.* **1983**, *95*, 579.
- (54) Ghanty, T. K.; Ghosh, S. K. *J. Phys. Chem.* **2002**, *106*, 11815.
- (55) Lee, H. M.; Kim, K. S. *J. Chem. Theory Comput.* **2009**, *5*, 976.
- (56) Gill, P. M. W.; Radom, L. *J. Am. Chem. Soc.* **1987**, *110*, 4931.
- (57) Sodupe, M.; Oliva, A.; Bertran, J. *J. Am. Chem. Soc.* **1994**, *116*, 8249.
- (58) Crawford, T. D.; Schaefer, H. F. *Rev. Comput. Chem.* **2000**, *14*, 33.
- (59) Rittby, M.; Bartlett, R. J. *J. Phys. Chem.* **1988**, *92*, 3033.
- (60) Purvis, G. D.; Bartlett, R. J. *J. Chem. Phys.* **1982**, *76*, 1910.
- (61) Scuseria, G. E. *Chem. Phys. Lett.* **1991**, *176*, 27.
- (62) Raghavachari, K.; Trucks, G. W.; Pople, J. A.; Head-Gordon, M. *Chem. Phys. Lett.* **1989**, *157*, 479.
- (63) Dunning, T. H. *J. Chem. Phys.* **1989**, *90*, 1007.
- (64) Kendall, R. A.; Dunning, T. H.; Harrison, R. J. *J. Chem. Phys.* **1992**, *96*, 6796.
- (65) Cremer, D. Møller-Plesset Perturbation Theory. In *The Encyclopedia of Computational Chemistry*; Schleyer, P. v. R., Allinger, N. L., Clark, T., Gasteiger, J., Kollmann, P. A., Schaefer, H. F., Schreiner, P. R., Ed.; Wiley: Chichester, 1998; Vol. 3, p 1706.
- (66) Shao, Y.; Fusti-Molnar, L.; Jung, Y.; Kussmann, J.; Ochsenfeld, C.; Brown, S. T.; Gilbert, A. T. B.; Slipchenko, L. V.; Levchenko, S. V.; O'Neill, D. P.; Distasio, R. A.; Lochan, R. C.; Wang, T.; Beran, G. J. O.; Besley, N. A.; Herbert, J. M.; Lin, C. Y.; Voorhis, T. V.; Chien, S. H.; Sodt, A.; Steele, R. P.; Rassolov, V. A.; Maslen, P. E.; Korambath, P. P.; Adamson, R. D.; Austin, B.; Baker, J.; Byrd, E. F. C.; Dachsels, H.; Doerksen, R. J.; Dreuw, A.; Dunietz, B. D.; Dutoi, A. D.; Furlani, T. R.; Gwaltney, S. R.; Heyden, A.; Hirata, S.; Hsu, C.-P.; Kedziora, G.; Khalliulin, R. Z.; Klunzinger, P.; Lee, A. M.; Lee, M. S.; Liang, W.; Lotyn, I.; Nair, N.; Peters, B.; Proynov, E. I.; Pieniazek, P. A.; Rhee, Y. M.; Ritchie, J.; Rosta, E.; Sherrill, C. D.; Simmonett, A. C.; Subotnik, J. E.; Woodcock, H. L.; Zhang, W.; Bell, A. T.; Chakraborty, A. K.; Chipman, D. M.; Keil, F. J.; Warshel, A.; Hehre, W. J.; Schaefer, H. F.; Kong, J.; Krylov, A. I.; Gill, P. M. W.; Head-Gordon, M. *J. Phys. Chem.* **2006**, *8*, 3172.
- (67) MOLPRO is a package of ab initio programs written by Werner, H. J.; Knowles, P. J.; Lindh, R.; Manby, F. R.; Schütz, M.; Celani, P.; Korona, T.; Rauhut, G.; Amos, R. D.; Bernhardsson, A.; Berning, A.; Cooper, D. L.; Deegan, M. J. O.; Dobbyn, A. J.; Eckert, F.; Hampel, C.; Hetzer, G.; Lloyd, A. W.; McNicholas, S. J.; Meyer, W.; Mura, M. E.; Nicklass, A.; Palmieri, P.; Pitzer, R.; Schumann, U.; Stoll, H.; Stone, A. J.; Tarroni, R.; Thorsteinsson, T.
- (68) Stanton, J. F.; Gauss, J.; Watts, J. D.; Lauderdale, W. J.; Bartlett, R. J. *Int. J. Quantum Chem.* **1992**, *44* (S26), 879.
- (69) Stanton, J. F.; Gauss, J.; Watts, J. D.; Szalay, P. G.; Bartlett, R. J.; with contributions from Auer, A. A.; Bernholdt, D. E.; Christiansen, O.; Harding, M. E.; Heckert, M.; Heun, O.; Huber, C.; Jonsson, D.; Jusélius, J.; Lauderdale, W. J.; Metzroth, T.; Michauk, C.; O'Neill, D. P.; Price, D. R.; Ruud, K.; Schiffmann, F.; Tajti, A.; Varner, M. E.; Vázquez, J.; and the integral packages: MOLECULE (Almlöf, J.; Taylor, P. R.), PROPS (Taylor, P. R.) and ABACUS (Helgaker, T.; Jensen, H. J. Aa.; Jørgensen, P.; Olsen, J.) ACESII; for the current version, see <http://www.aces2.de>.
- (70) Crawford, T. D.; Sherrill, C. D.; Valeev, E. F.; Fermann, J. T.; King, R. A.; Leininger, M. L.; Brown, S. T.; Janssen, C. L.; Seidl, E. T.; Kenny, J. P.; Allen, W. D. *J. Comput. Chem.* **2007**, *28*, 1610.
- (71) Yamaguchi, Y.; Alberts, I. L.; Goddard, J. D.; Schaefer, H. F. *Chem. Phys.* **1990**, *147*, 309.
- (72) Crawford, T. D.; Stanton, J. F.; Allen, W. D.; Schaefer, H. F. *J. Chem. Phys.* **1997**, *107*, 10626.
- (73) Burton, N. A.; Yamaguchi, Y.; Alberts, I. L.; Schaefer, H. F. *J. Chem. Phys.* **1991**, *95*, 7466.
- (74) Jensen, P.; Bunker, P. R. *Computational molecular spectroscopy*; John Wiley & Sons, LTD.: New York, 2000.
- (75) Szabo, A.; Ostlund, N. S. *Modern Quantum Chemistry: Introduction To Advanced Electronic Structure Theory*; Dover: New York, 1998.
- (76) Reed, A. E.; Weinstock, R. B.; Weinhold, F. *J. Chem. Phys.* **1985**, *83*, 735.
- (77) Reed, A. E.; Weinhold, F. *J. Chem. Phys.* **1983**, *78*, 4066.
- (78) Sodupe, M.; Bertran, J.; Rodriguez-Santiago, L.; Baerends, E. J. *J. Phys. Chem.* **1999**, *103*, 166.